ENHANCEMENT ON THE THERMAL BEHAVIOR USING HEAT PIPE ARRAYS IN BATTERY THERMAL MANAGEMENT COMPARED TO COOPER RODS

by

Chaoyi WAN*

School of Automobile and Traffic Engineering, Jiangsu University of Technology, Changzhou, Jiangsu, China

Original scientific paper
https://doi.org/10.2298/TSCI191210124W

In the present study, the thermal behavior of a power battery cooling structure employing copper rods, and heat pipes was compared. The influences of flow rate and inlet temperature of coolant, as well as input power were discussed by numerical methods. The numerical computation results showed that heat pipe could significantly augment the heat transfer of the battery cooling system than the copper rod. Within the scope of this study, the heat pipe reduced the maximum temperature by 41.6-60.9%. The distributions of temperature ratios on the battery surface, together with the heat flux as soon as streamlines around the heat pipe condenser was also illustrated.

Key words: *battery thermal management, heat pipe, temperature differences, heat transfer enhancement*

Introduction

Currently, the lithium-ion battery should be the most promising energy storing equipment for hybrid electric vehicles or electric vehicles for its tremendous energy density [1, 2]. However, the optimum working temperature for the lithium-ion battery is limited in the scope of 25-40 °C [3-6], and maximal temperature difference should not exceed 5 °C in one battery pack [7, 8], otherwise, it may cause serious safety problems [6, 7]. The heat pipe cooling system which uses liquid-gas phase change without consuming extra power has become the most promising cooling method for with the excellent heat transfer performance and rapid response capability in lithium-ion batteries thermal management system [3, 4, 9, 10].

The power battery generates heat more than 50 W [11, 12], and more during acceleration and other high charging or discharging conditions. Rao *et al.* [4] conducted experimental research which shows the highest temperature of the battery surface would be restricted not above 50 °C when thermal load is under 50 W. Yet the peak value of temperature differences is about 8 °C. The heat load should not exceed 30 W to retain the surface temperature differences within 5 °C. An experiment studied of Wang *et al.* [13] mentioned that the temperature of battery surface can stay within 70 °C during heat generation per cell lasts between 20-40 W. Or the amount of heat generation cannot exceed 10 W in order to the maximum temperature below 40 °C. Ye *et al.* [11] found the heat transfer coefficient on the condenser surface decreased significantly along flow passage, and causing unevenness of the battery temperature. Dummy heat pipes and copper fins

* Author's e-mail: wina-1@163.com

could enhance the heat transfer and temperature uniformity. Ye *et al.* [14] also pointed out that the addition of fins on heat pipe condenser surfaces have such considerable consequence on lowering the maximum temperature along with the temperature differences on battery surface.

More information is needed to investigate the influence of parameters of the heat pipe for lithium-ion batteries thermal management. Within this paper numerical investigations were carried on about flow details and heat transfer characteristics in a heat pipe cooling structure applying for the high-power Li-ion battery. Reliability of the computation models and meshes used in this investigation was carefully tested and calibrated by comparing with experimental data in the literature. Amounts of indicators such as temperature, heat flux, and pressure loss were extracted to characterize the heat behavior of heat pipe cooling system.

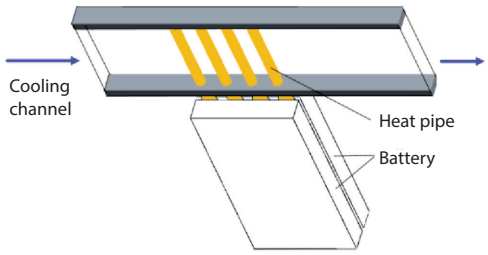

Figure 1. The configuration of the heat pipe cooling structure applying for prismatic battery packs

Numerical set-up

Geometry models and simplifications

A configuration of the heat pipe cooling structure for a prismatic battery pack is displayed in fig. 1.

In-between two prismatic batteries (118 × 63 × 13 mm) is sandwiched the evaporator sections of four heat pipes. The thermal which is produced from the battery could be transferred to the condenser section through the gas-liquid phase change in heat pipe and then emitted into coolant flow through the cooling passage (300 × 60 × 12 mm). Each heat pipes were flattened from tubular condenser (Φ = 6.0 mm) to rectangular evaporator section (2.0 × 8.5 mm). Table 1 listed the structure parameters of batteries and the cooling channel. The copper cooling system is designed as similar except that the heat pipes are turned to pure copper rods. Cross-section radius of vapor core is 0.002 m. The entire heat pipe is 0.198 m long. The porosity of the wick region is 0.50.

Table 1 Parameters of the heat pipe arrays for the prismatic battery

Parameters of the heat pipe arrays for the prismatic battery		
l_t	The total length of the heat pipe [m]	0.198
l_c	Length of condenser section [m]	0.06
l_{ad}	Length of adiabatic section [m]	0.02
l_e	Length of evaporator section [m]	0.118
r_c	Cross section radius of copper shell [m]	0.003
r_i	Inner chamber radius of wick region [m]	0.0026
r_v	Cross section radius of vapor core [m]	0.002
ε	Porosity [–]	0.50

It is complex and time-consuming to model all details for a battery pack or module cooled by heat pipe for phase changes and other phenomena in heat pipes. Even on the condition of simulating one heat pipe, high computational resources are necessitated to characterize the mass transfer and heat transfer while in process of transient charging or discharging of the cell. Thus, one more efficient approach for numerical computation is adopted. The thermal behavior of a heat pipe on battery cooling would be treated as a thermal network assembled

by various segments, and then first-order linear ordinary differential equation can describe this transient characteristic [15]. Additionally, solving electro-chemical reactions of a battery is also too complicated for only presenting the thermal behavior of battery cell (multi-layer structure). Therefore, a simplified model without considering electro-chemical reactions is applied to present the heat produced by the battery, as well as the thermal properties of a multi-layered battery cell. This approach is well certified by comparisons between experimental and numerical researches and is applied in many pieces of literature [1, 9, 11, 15].

Model formulation of the heat pipe

Copper shell

During the simulation, the physical and thermal properties of copper were applied directly to the shell because heat transfer through the copper shell of the heat pipe is entirely conduction.

Wick region

The heat pipe selected in this present study has a maximal heat transfer limit over the target thermal load to avoid drying during operation. The wick region was considered as a porous media filled of distilled water. A widely confirmed model established by Chi *et al.* [16] was employed to determine the effective thermal conductivity of the wick region k_{wick}:

$$k_{\text{wick}} = \frac{k_l[(k_l + k_s) - (1-\varepsilon)(k_l - k_s)]}{[(k_l + k_s) + (1-\varepsilon)(k_l - k_s)]} \tag{1}$$

where k_l and k_s are the thermal conductivity, respectively, of working medium and the porous wick, and ε is the porosity. In this research, here the effective thermal conductivity in the wick region was calculate as 1.814 W/mK.

The sintered copper powder porous wick and distilled water were volumetric averaged to be utilized to determine to the density of the wick region, and the specific heat capacity is obtained, respectively:

$$\rho_{\text{wick}} = \varepsilon\rho_l + (1-\varepsilon)\rho_s \tag{2}$$

$$C_{\text{wick}} = \frac{[\varepsilon\rho_l C_l + (1-\varepsilon)\rho_s C_s]}{\rho_{\text{wick}}} \tag{3}$$

where ρ_{wick}, ρ_i, ρ_s are, respectively, wick region density, working fluid density, and the copper powder density. The ε is the porosity of the wick. Moreover, C_{wick}, C_l, C_s are, respectively, the specific heat capacity of the wick, the working fluid, and the copper powder.

Vapor core

The vapor flow was considered incompressible, laminar and fully developed. In a tubular heat pipe, by assuming the relationship between pressure drop and temperature drop based upon the the ideal gas law as well as Clapeyron equation, we calculate the effective thermal conductivity of the vapor core [17, 18]:

$$k_{\text{vapor}} = \frac{r_v^2 L^2 \rho P_v}{8\mu \text{R} T^2} \tag{4}$$

where r_v is the cross-sectional radius of the heat pipe vapor core, L – the latent heat of working fluid, ρ – the density, P_v – the saturation pressure, μ – the dynamic viscosity, R – the gas constant, and T – the water vapor temperature. The k_{vapor} was determined as $4.69 \cdot 10^6$ W/mK employing the physical parameters of saturated water vapor at 40 °C.

Thermal model for the battery

Two aluminum blocks of the same size as some commercial power battery were used to simulate batteries [4, 13, 19, 20]. It is assumed that in the whole operation procedure, the heat generation rate within the cell is considered as a constant value which is regarded as the maximum power during the highest sustainable constant-current discharge rate. Within the present research, the thermal load is in the range of 20-80 W per cell.

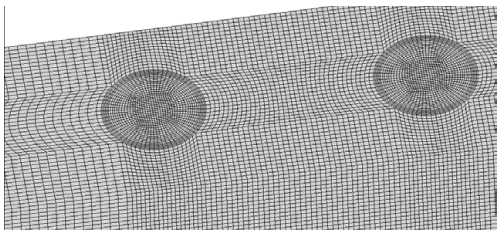

Figure 2. The hexahedral mesh used in the present numerical study

Numerical procedures

In this calculation, numerical studies were performed by the commercial CFD software ANSYS Workbench 17.2 FLUENT using a local parallel solver in a double-precision mode. Heat radiation transfer is negligible and was not considered.

Block-structured meshes composited by hexahedral elements were employed for realizing the spatial discretization of the computational domain. Cell orthogonality was ensured by introducing multiple O-grid blocks for heat pipes. Denser girds were applied in the non-slip boundary regions where the gradients of flow and temperature are greater, *i. e.*, the area around heat pipes and the end wall of the coolant channel. The grid independence test was performed by gradually refining the mesh size (in this study, three different meshes containing 2628477, 4737970, and 7895174 cells, respectively) to ensure that the mesh size has little impact on the results. The control parameter was for grid independence test was the highest temperature of the cell surface. According to the procedure described [21], the grid convergence index was 2.81%. Figure 2 shows the mesh used in this numerical investigation.

Model validation

The results obtained by the computation procedure were well compared with the published experimental data of Liang *et al*. [20]. All materials, boundary conditions, and data processing methods are modified according to the experiment of Liang *et al*. [20]. The computation models coupled the heat transfer in the solid and fluid to solve energy equations automatically. The surface of the channel and the insulation section of heat pipes are treated as isolation and no-slip boundaries. The two batteries have a constant volume heat generation rate. At the inlet of the channel, constant velocity was applied. Laminar is used to calculate the viscous due to the inlet Reynolds number. Data are plotted in fig. 3 for comparison. As illustrated, the maximal deviation between numerical computation results in this research and data from [20] were kept within 10%. Thus, the numerical model is considered to be reliable to applied to forecast the heat characteristic of such heat pipe cooling system based on the above validation.

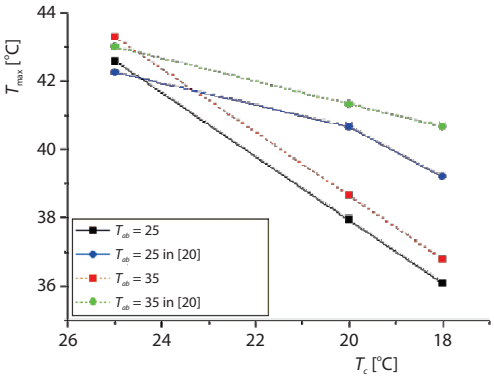

Figure 3. Results of maximum temperature varied with coolant inlet temperature obtained by CFD and experimental data from Liang *et al*. [20] for comparison

Results and discussion

Effects of flow rate

In this part, effects on coolant flow rate of the battery surface temperature while using heat pipes and copper rods is compared. The input power represent the heat generated from the battery is set at 40 W/cell while the coolant inlet temperature T_c is set as 25°C. The cooling flow rate for studied ranges of 0.5-8 Lpm. The maximum temperature, T_{max}, averaged temperature, T_{avg}, and temperature differences, ΔT, of battery surface with different coolant flow rates for both configurations are shown in fig. 4.

The trend of T_{max} and T_{avg} for both heat pipe and copper rod is similar. At first, the T_{max} and T_{avg} reduced rapidly with the increased flow rate until 2 Lpm then gradually be gentle. The temperature differences of the cell surface ΔT almost keep constant.

While the flow rate varies between 0.5 and 8 Lpm, the maximal temperature on the battery surface cooled by copper rod changes from 107.81-84.24 °C, decreased by 21.9%, and that by heat pipe changes from 52.74-39.77 °C, decreased by 24.6%. The heat pipe reduced the maximum temperature by 51.1-52.8%. While the volume flow rate changes from 0.5-8 Lpm, and temperature differences by copper rod changes from 19.34-18.51 °C, and that by heat pipe changes from 2.08-1.74 °C. The heat pipe reduced the maximum temperature by 89.3-90.6%. Compared to copper rods, heat pipes significantly diminish the maximal temperature as well as temperature differences on battery surface.

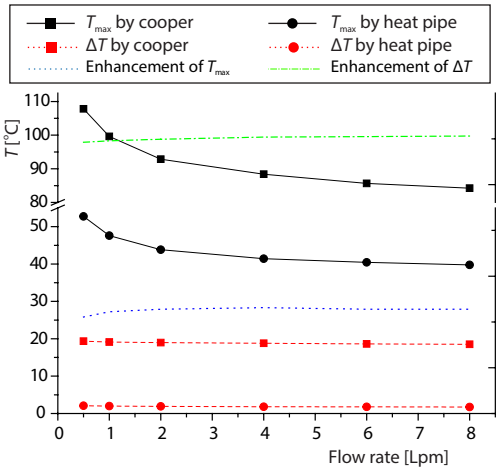

Figure 4. The T_{max}, T_{avg}, and ΔT of battery with different coolant flow rates (T_c = 25 °C while input power is 40 W/cell)

Effect of inlet temperature

In this part, the input power represented the battery thermal load is applied to 40 W/cell when the flow rate is a constant value of 2 Lpm to inspect influence upon the inlet temperature of such cooling construction. The coolant inlet temperature ranges from 25-45 °C. The maximum temperature, T_{max}, averaged temperature, T_{avg}, and temperature differences, ΔT, on battery surface with different coolant inlet temperatures by copper rod and heat pipe is displayed in fig. 5.

Both T_{max} and T_{avg} by cooper rod and heat pipe increase linearly as coolant inlet temperature increases. As coolant inlet temperature increases from 15-35 °C, the maximum temperature T_{max} of copper rod increases from 82.85-102.85 °C, the enhancement is 24.1%,

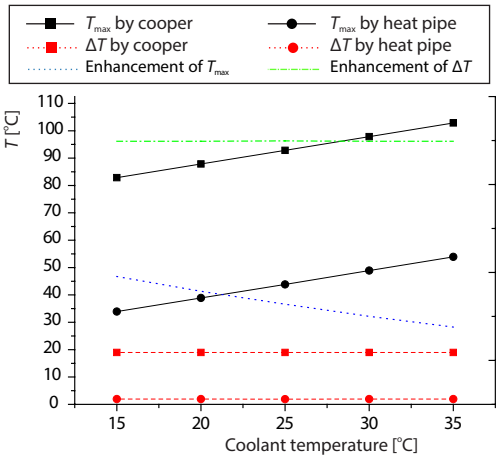

Figure 5. The T_{max}, T_{avg}, and ΔT of battery with different coolant inlet temperatures (input power is 40 W/cell under q_v = 2 Lpm)

and the data of heat pipe is from 33.91-53.91 °C, the enhancement is 59.0%. The heat pipe reduced the maximum temperature by 59.1%-47.6%. The temperature uniformity is less affected by coolant inlet temperature. The temperature differences, ΔT, is always around 19.0 °C and 1.9 °C. The heat pipe reduced the maximum temperature by 89.8%. Compared to copper rods, heat pipes significantly lessen the maximum temperature and temperature differences.

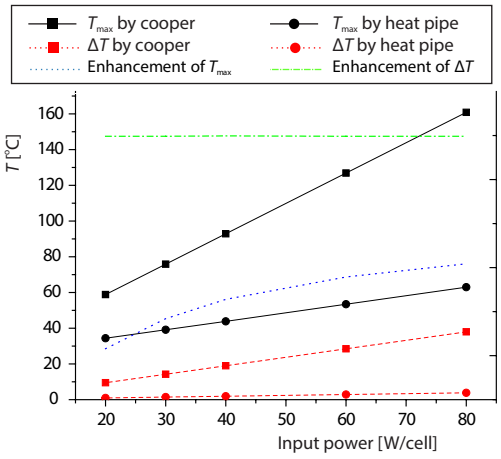

Figure 6. The T_{max}, T_{avg}, and ΔT of battery with different input power(mass-flow rate q_v = 2 Lpm under coolant inlet temperature T_c = 25 °C)

Effect of input power

In this part, the impact of input power on the temperature of the surface cooled by cooper rod and heat pipe is studied. The cooling flow rate is fixed to be 2 Lpm under T_c = 25 °C, and the input power ranges from 20-80 W. The maximum temperature, T_{max}, averaged temperature, T_{avg}, and temperature differences, ΔT, of battery surface with different input powers of this battery are demonstrated as follows in fig. 6.

As displayed, T_{max} , and T_{avg} as well as ΔT significantly increases as the input power increases. While the input power changes from 20-80 W, the maximum temperature of copper rod increases from 58.84-160.85 °C, enhancement 173.4% and that data of heat pipe increases from 34.38-62.97 °C， increasement 83.2%. The heat pipe reduced the maximum temperature by 41.6%- 60.9%. The temperature differences of copper rod increases from 9.49-37.96 °C, and that data of heat pipe increase from 0.96-3.86 °C. The heat pipe reduced the maximum temperature by 89.8%.

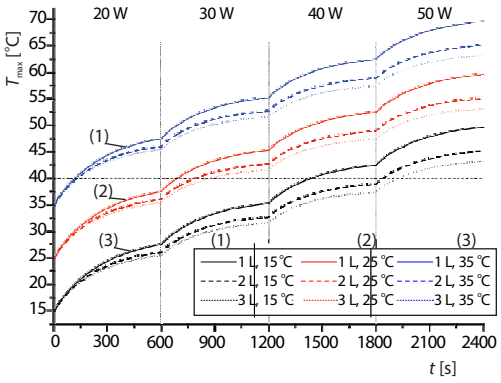

Figure 7. Temperature response of battery with varied flow rates under varied coolant inlet temperature

Transient characteristic of heat pipe

For further studying the characteristics of heat pipes, transient responses were also investigated. Influences of the flow rate and inlet temperature of the heat pipe system of cell surface temperature is examined. The maximum temperature, T_{max}, of battery surface with different flow rates and inlet temperatures under varied input powers processes is shown in fig. 7. The cooling flow rate for studied ranges from 1-3 Lpm, and the inlet temperature ranges between 15-35 °C. The input power changes every 600 seconds from 20-50 W while in each period it almost keep constant. Initial temperature of the cooling system and battery fixed at the same as coolant inlet temperature in each condition.

As fig. 7 illustrated, T_{max} increased with the input power and coolant inlet temperature and decreased with the rising coolant flow rate. However while it is increasing, the reduction of T_{max} gradually decreased. It is worth noting that the temperature difference hardly changes with coolant inlet temperature.

Temperature response of battery at coolant flow rate q_v = 2 Lpm under varied coolant inlet temperature is displayed in fig. 8. According to fig. 8, even at the thermal production amount of 50 W/cell within the scope of this study T_{max} is always below 40 °C while T = 15 °C. The T_{max} is also below 40 °C while T_c = 25 °C with thermal production rate below 30 W/cell. However T_{max} exceed 40 °C even while the thermal production amount is at 20 W/cell.

Figure 9 shows the equilibrium T_{max} of cell surface under varied coolant inlet temperatures, flow rate and varied cell thermal load.

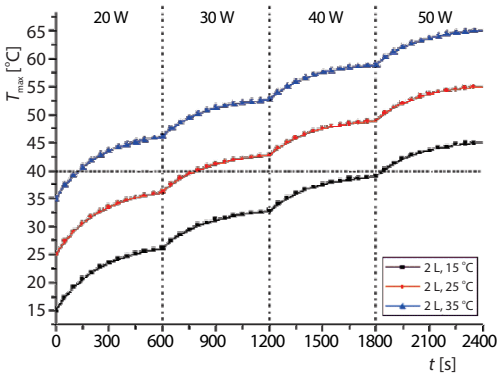

Figure 8. The T_{max} response of cell variation with varied input powers and coolant inlet temperature (q_v = 2 Lpm)

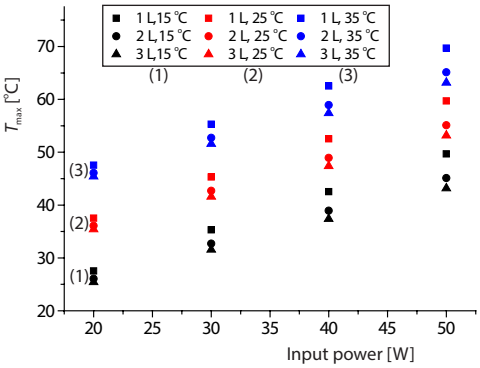

Figure 9. The equilibrium T_{max} of cell surface under varied coolant inlet temperatures, coolant flow rate and varied input power

Conclusions

Within the present investigation, the thermal behavior of this power battery cooling system adopting copper rods and heat pipes was compared. The influences of flow rate, inlet temperature of coolant, as well as input power were discussed by numerical methods. Numerical models and procedures are carefully validated and calibrated with experimental results in the literature. The model and approach demonstrated considerable accuracy and was then employed to sensitivity analysis. Amounts of indicators such as temperature, heat flux, and pressure loss were extracted to characterize the heat conduction and convection feature of the cooper rod and heat pipe cooling system. Outcomes can provide some useful guidance for understanding the cooling mechanism of heat pipe. Several major conclusions can be drawn as follows.

- Compared to copper rods, heat pipes significantly diminish the maximal temperature as well as temperature differences on the battery surface, respectively by 41.6%-60.0% and 89.8%-90.6%.
- The distributions of the temperature ratio T/T_{avg} display the heat transfer uniformity of the battery surface, together with the heat flux and streamlines, respectively on the copper rod and heat pipe condenser explains the effect of flow rate, inlet temperature of coolant, as well as input power on the behavior of the heat pipe cooling system.

Acknowledgment

This work was supported by the Natural Science Foundation of Jiangsu Province (Grants No. BK20170317).

References

[1] Choi, Y. S, Kang, D. M., Prediction of Thermal Behaviors of an Air-Cooled Lithium-Ion Battery System for Hybrid Electric Vehicles, *Journal of Power Sources*, *270* (2014), Dec., pp. 273-280
[2] Etacheri, V., *et al*., Challenges in the Development of Advanced Li-Ion Batteries: A Review, *Energy and Environmental Science*, *4* (2011), 9, pp. 3243-3262
[3] Tran, T.-H., *et al*., Experimental Investigation on Heat Pipe Cooling for Hybrid Electric Vehicle and Electric Vehicle Lithium-Ion Battery, *Journal of Power Sources*, *265* (2014), Nov., pp. 262-272
[4] Rao, Z., *et al*., Experimental Investigation on Thermal Management of Electric Vehicle Battery with Heat Pipe, *Energy Conversion and Management*, *65* (2013), Jan., pp. 92-97
[5] Waldmann, T., *et al*., Temperature Dependent Ageing Mechanisms in Lithium-Ion Batteries – A Post-Mortem Study, *Journal of Power Sources*, *262* (2014), Sept., pp. 129-135
[6] Bandhauer, T. M., A Critical Review of Thermal Issues in Lithium-Ion Batteries, *Journal of the Electrochemical Society*, *158* (2011), 3, pp. R1-R25
[7] Troxler, Y., *et al*., The Effect of Thermal Gradients on the Performance of Lithium-Ion Batteries, *Journal of Power Sources*, *247* (2014), Feb., pp. 1018-1025
[8] Wang, T., *et al*., Thermal Investigation of Lithium-Ion Battery Module with Different Cell Arrangement Structures and Forced Air-Cooling Strategies, *Applied Energy*, *134* (2014), Dec., pp. 229-238
[9] Greco, A., *et al*., A Theoretical and Computational Study of Lithium-Ion Battery Thermal Management for Electric Vehicles Using Heat Pipes, *Journal of Power Sources*, *257* (2014), July, pp. 344-355
[10] Rao, Z., *et al*., Experimental Study of an OHP-Cooled Thermal Management System for Electric Vehicle Power Battery, *Experimental Thermal and Fluid Science*, *57* (2014), Sept., pp. 20-26
[11] Ye ,Y., *et al*., Numerical Analyses on Optimizing a Heat Pipe Thermal Management System for Lithium-Ion Batteries during Fast Charging, *Applied Thermal Engineering*, *86* (2015), July, pp. 281-291
[12] Ye, Y., *et al.*, Effect of Thermal Contact Resistances on Fast Charging of Large Format Lithium Ion Batteries, *Electrochimica Acta*, *134* (2014), July, pp. 327-337
[13] Wang, Q., *et al*., Experimental Investigation on EV Battery Cooling and Heating by Heat Pipes, *Applied Thermal Engineering*, *88* (2015), Sept., pp. 54-60
[14] Ye, Y., *et al*., Performance Assessment and Optimization of a Heat Pipe Thermal Management System for Fast Charging Lithium Ion Battery Packs, *International Journal of Heat and Mass Transfer*, *92* (2016), Jan., pp. 893-903
[15] Zuo, Z., Faghri, A., A Network Thermodynamic Analysis of the Heat Pipe, *International Journal of Heat and Mass Transfer*, *41* (1998), 11, pp. 1473-1484
[16] Chi, S., *et al.*, *Heat Pipe Theory and Practice: A Sourcebook*, John Wiley and Sons Inc., New York, USA, 1976
[17] Prasher, R. S., A Simplified Conduction Based Modelling Scheme for Design Sensitivity Study of Thermal Solution Utilizing Heat Pipe and Vapor Chamber Technology, *Journal of Electronic Packaging*, *125* (2003), 3, pp. 378-385
[18] Wei, X., Sikka, K., Modelling of Vapor Chamber as Heat Spreading Devices, *Proceedings*, Proceedings of the Thermal and Thermomechanical, *Proceedings*, 10th Intersociety Conference on Phenomena in Electronics Systems, San Diego, Cal., USA, 2006, Vol. 2, pp. 231-238
[19] Ling, Z., *et al*., Experimental and Numerical Investigation of the Application of Phase Change Materials in a Simulative Power Batteries Thermal Management System, *Applied Energy*, *121* (2014), May, pp. 104-113
[20] Liang, J., *et al*., Investigation on the Thermal Performance of a Battery Thermal Management System Using Heat Pipe under Different Ambient Temperatures, *Energy Conversion and Management*, *155* (2018), Jan., pp. 1-9
[21] Celik, I., *et al*., Procedure for Estimation and Reporting of Uncertainty Due to Discretization in CFD Applications, *Journal Fluids Eng*., *130* (2008), 7, 078001

Paper submitted: December 10, 2019
Paper revised: January 17, 2020
Paper accepted: February 3, 2020